Finite Element Analysis for Post-Cracking Design of Thermal Well Cements

Jueren Xie

C-FER Technologies, Canada

Abstract: *Steam Assisted Gravity Drainage (SAGD) and Cyclic Steam Stimulation (CSS) are typical thermal well technologies used for the recovery of heavy oil and oil sands resources. Cyclic thermal loading, resulting from temperature variation with the peak operating temperatures in the range of 220°C to 350°C, often subjects the well cement sheath to significant longitudinal and circumferential tensile or compressive stresses, leading to potential failure modes, including cracking, crushing and de-bonding. Failure of cement sheath would compromise the well and caprock integrities. Therefore, ensuring satisfactory performance of cement sheath over the well life has been one of the key challenges in thermal well designs.*

Traditional well design uses the stress-based design concept which limits the longitudinal and circumferential cement stresses to the tensile strength value. The stress-based design has been proven to be overly conservative and often impossible to meet for thermal well cements. For developing a more suitable design criterion, advanced finite element analysis (FEA) modeling techniques are required to capture the complex cement behavior in thermal wells.

This paper presents an FEA approach by using a damaged plasticity model to capture the complex thermal and mechanical behavior of cement material. The damaged plasticity model considers the thermal conductivity, tri-axial stress effect, strain-hardening due to plasticity, strain-softening due to cracking and cyclic loading responses. This paper also presents a post-cracking design concept as a new design basis to allow limited cement cracking, providing that the permeability of the cement remains within an acceptable limit. An illustrative example is presented to demonstrate the use of FEA approach and post-cracking design concept for the design of thermal well cements.

***Keywords**: Casing, Cement, Compressive Strength, Cooling, Cooling Rate, Damage, Cracking, Finite Element Analysis (FEA), Heating, Heating Rate, Monte Carlo Simulation, Plasticity, Tensile Strength, Thermal Cement, Thermal Cycle, Thermal Well, Young's modulus*

1. Introduction

Operation of thermal wells presents cyclic thermal loading resulting from temperature changes, with the peak steam temperature in the ranges from 220°C to 275°C for SAGD wells and from 330°C to 350°C for CSS wells. When the steam is first injected into the wells, steep thermal gradients across the cement sheath may develop due to the large temperature difference between the steam and the surrounding formations. Casing material, with the high thermal conductivity and a high coefficient of thermal expansion of steel, tends to expand quickly, subjecting the relatively cold cement sheath to tensile circumferential stresses. As the cement material typically has a low tensile strength, the thermal expansion of casing during heating can potentially cause the cement sheath to crack. In the cooling phase, as a result of well shut-in, the difference in thermal contraction of casing, cement and formation material may also cause loss of the cement bond to the casing string. Cement cracking and de-bonding may allow for fluid migration along the well, which may compromise the hydraulic isolation role of the cement sheath. This is often of special concern in the caprock region, as axial cracking through this zone could allow steam and hydrocarbons to migrate to overlying formations, or even to surface. Cement cracking and de-bonding also present concerns for potential Stress Corrosion Cracking (SCC) for casing string. To consider the impact of thermal load, thermal wells require the use of thermal cement, which according to the Alberta Energy Regulator (AER) is a blend which does not exhibit a significant reduction in strength when subjected to temperatures greater than 360°C (AER, 1990).

Traditionally, a stress-based design concept is used in designing well cement. This approach limits the tensile stress in the cement sheath to the tensile strength of the material to prevent the occurrence of cement cracking. To determine the stress conditions in the cement sheath, several FEA studies have been carried out by various investigators (e.g. Thiercelin, 1997; Bosma, 1999; Ravi, 2008). Some early FEA studies used thermo-elastic material and one- or two-dimensional structural models. Use of such models may disregard the tri-axial stress conditions and Poisson's ratio effects in the cement. Since stress-based design has been typically used, little effort has made in modeling the non-linear material behavior, such as yielding of the casing and yielding, crushing and cracking of the cement sheath. The Mohr-Coulomb material model used by some may simulate cement failure by the application of a shear failure criterion; however, this approach appears to overlook the effects of cement cracking and crack propagation.

Xie et al. (2011) used a smeared cracking model implemented by Abaqus to investigate the impact of heating rate on the cracking potential of the cement sheath during the heating phase for SAGD wells. The smeared cracking constitutive model simulated the cracking and crushing behavior of the cement material under monotonic loading (e.g. heating operation). One of the shortcomings of this study was that the analyses were limited to the heating phase of thermal operations and the cement response to cyclic thermal loading was not analyzed.

This paper presents a review of cement mechanical properties and proposes a new design basis: post-cracking design concept. To facilitate the use of the post-cracking design approach, a damaged plasticity model is recommended to capture the thermal-mechanical behavior of cement in thermal wells. The damaged plasticity model uses the plasticity theory to consider the tri-axial stress effect, strain-hardening due to plasticity, strain-softening due to cracking and cyclic loading. An analysis example is presented in the paper to show the impact of heating and cooling loading on cement performance.

2. CEMENT MECHANICAL PROPERTIES

Comprehensive FEA models often require the use of the stress-strain material responses under uniaxial tensile and compressive loading. Schematic representations of such responses are shown in Figure 1. Mechanical properties for cement materials include elastic modulus, Poisson's ratio, tensile strength, compressive strength, fracture energy and thermal expansion coefficient (MacGregor, 1992; Xie et al., 1995). These properties often vary with temperature. The key thermal properties include the thermal conductivity and specific heat.

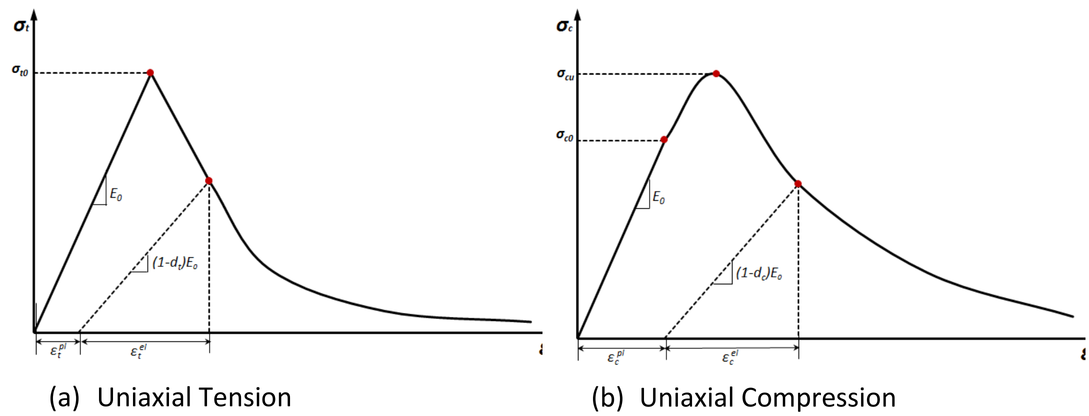

Figure 1 Schematic Representation of Stress-Strain Relationships in Cement under Uniaxial Tension and Uniaxial Compression

2.1 Key Mechanical Parameters

Table 1 presents a list of key mechanical parameters such as elastic modulus, Poisson's ratio, compressive strength and tensile strength.

Dean et al. (2002) showed a type of API Class G cement with Young's modulus of 3.1 GPa and compressive strength of 6.9 MPa.

Stiles (2006) studied the mechanical properties of five cement formulations after exposure to a temperature of 340°C. The five formulations were: 1) conventional Class G; 2) thixotropic system (Class A); 3) foamed Class G; 4) high strength and low density system; and 5) flexible and expanding low density system. Stiles determined that the mechanical properties change significantly after 24 months of curing at temperature and the degree of changes vary among cement formulations. The key mechanical properties determined by Stiles, corresponding to the five formations were: elastic modulus of 7.3, 2.3, 4.0, 6.5 and 4.2 GPa before curing; 12.1, 6.8, 6.1, 1.4 and 1.4 GPa after 24 months curing; effective compressive strengths of 32.3, 15.5, 23.1, 48.9 and 37.2 MPa before curing; ;56.2, 40.7, 28.3, 11.9 and 13.8 MPa after curing; tensile strengths of 2.6, 2.3, 2.6, 3.2 and 2.2 MPa before curing; and 7.3, 6.4, 4.5, 1.6 and 1.5 MPa after curing.

DeBruijn et al. (2009) performed a study of SAGD well integrity using three cement formulations: flexible cement, thixotropic cement and conventional thermal cement. The key mechanical properties considered which correspond to these three cements were: elastic modulus values of 2.1, 5.5, 8.5 GPa; compressive strengths of 9, 28.8 and 48 MPa; and tensile strengths of 1.2, 4.4 and 4.8 MPa.

Table 1. Description of Key Mechanical Parameters for Cement.

Parameter	Description
Elastic modulus (E_c)	It is a measure of stiffness during the initial elastic deformation under tensile or compressive loading. The elastic modulus in tension is often assumed to be the same under compression.
Poisson's ratio (v)	It is the ratio of transverse to axial strain
Compressive strength (f_c')	It refers to the uniaxial compressive strength as measured by a compressive test of a standard test cylinder of cement. The effect of confinement on cement compressive stress-strain response should also be considered. Generally, the radial confining stress increases the compressive strength and post-peak stress level. Tri-axial stress tests can be performed using a tri-axial Hoek cell (Xie et al., 1995).
Tensile strength, (f_t',)	It is taken to refer to the cement strength under uniaxial tensile loading. It is, however, often determined through a flexural test of a plain cement beam or a split cylinder test, rather than the direct uniaxial tension test.

2.2 Cement Cracking and Fracture Energy

Fracture mechanics based FEA was first presented by Hillerborg et al. (1976) for concrete and cement materials. The key assumption was that the stresses act across a crack as long as it is narrowly opened. The mechanical response during the narrowly opened cracking phase is called strain-softening. In order to capture the cracking and strain-softening behavior, Hillerborg et al. (1976) proposed the use of fracture energy value in the FEA model.

There are two alternative test approaches to quantify the strain softening and fracture energy of cement in tension: the direct tension test and the flexural test on notched beams (Xie et al., 1995). Both types of tests must be conducted with the testing machine in stroke control to capture the descending part of the load-deflection response. Figure 2 presents schematics of tensile stress versus cracking-displacement relationship. The dashed curve shows the typical variation from coupon tests. In FEA modeling, such a relationship is often simplified by a linear curve, shown in Figure 2 as the solid line. The area underneath the tensile stress-displacement curve is called the fracture energy,(G_f) as defined by Hillerborg et al. (1976).

Macharia et al. (2011) determined that the fracture energy values of Portland blast furnace cement were in the range of 0.138 to 0.211 N/mm for dry samples and 0.117 to 0.150 N/mm for sealed samples. Padevet and Zobal (2011) found significantly higher values of fracture energy for cement paste with fly ash.

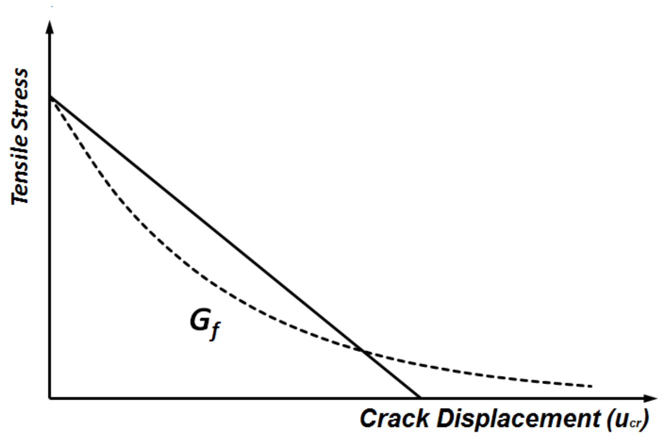

Figure 2 Schematic Representation of Stress vs. Cracking Displacement Response and Fracture Energy of Cement

2.3 Creep

Creep is the permanent, time-dependent deformation to relieve stresses within the cement material. Cement that is subjected to sustained forces over long-durations is prone to creep. Creep may reduce the effects of cracking that occurs in cement; however, this effect requires further validation through testing.

3. POST-CRACKING DESIGN CONCEPT

Traditionally, the stress-based design approach was used which limited the tensile stress in the cement sheath to the tensile strength of the material to prevent the occurrence of cement cracking. However, the tensile strength limit requirement appears to be stinging, as the typical heating operation inevitably imposes initial cracking in the cement sheath in thermal wells (Xie et al, 2011). In an effort to develop a more reasonable design criterion, a post-cracking design concept was recently proposed (Xie, 2014a, 2014b and 2015). The post-cracking design concept was based on the fracture mechanics by Hillerborg et al. (1976) who considered that the stresses act across a crack for cement type materials, as long as the crack opening is narrow. Therefore, one can postulate that the permeability of cement materials may be affected by the initial cracking; however, this effect would not be significant until the cracks open widely. The post-cracking design concept allows the use of cement beyond the tensile strength limit, as long as the crack width (i.e. crack displacement) in the cement is limited.

The post-cracking design criterion can be described as:

$$u_{cr} \leq (u_{cr})_{allowable}$$

where u_{cr} is the crack displacement and (u_{cr} allowable) is the allowable crack displacement. The crack displacement can be determined from FEA, while the allowable crack displacement should be determined from physical tests.

The crack displacement threshold can be defined by controlling the permeability to an acceptable level, while maintaining sufficient residual strength of the material for potential further loading.

The permeability of cracked cement and concrete materials has been studied by several investigators (Wang, Jansen and Shah, 1997, Picandet, Khelidj and Bellegou, 2009, Akhavan, Shafaatian and Ajabipour, 2013, Walsh, et al., 2012; Abdoulghafour, et al., 2013). Figure 3 shows the schematic representation of the relationship between permeability (in logarithm scale) and crack width, based on the review of published work on cement and concrete materials.

The work, completed by Wang, Jansen and Shah (1997) suggested that for a cracked concrete sample, after unloading, the water permeability coefficient increased from 1×10^{-9} cm/s to 1×10^{-6} cm/s (as the crack opening displacement increased from 0 to 50 microns); however, the water permeability coefficient increased from 1×10^{-6} cm/s to 1×10^{-3} cm/s as the crack opening displacement increased from 50 to 200 microns. The key finding of the study was that the concrete crack opening had little effect on permeability if the cracking opening displacement was less than 50 microns.

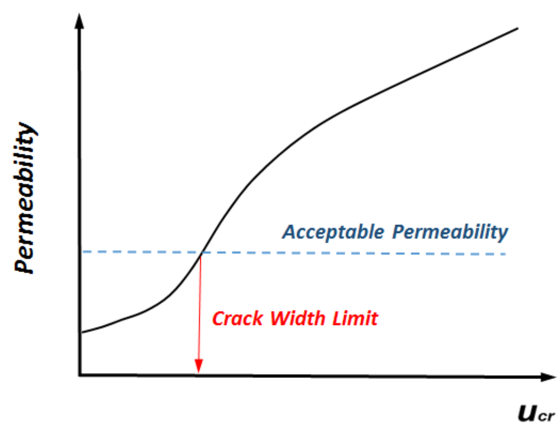

Figure 3 Schematic Representation of Permeability and Crack Width Relationship

In the light of the work completed by Wang, Jansen and Shah (1997), this paper uses 25.4 microns as the crack width limit for the post-cracking design for cements, allowing for the design of cements beyond tensile strength limit while controlling the permeability to a reasonable low level. The threshold is expressed as:

$$(u_{cr})_{allowable} = 25.4 \text{ Microns}$$

Macharia et al. (2011) determined that the fracture energy values of Portland blast furnace cement were in the range of 0.138 to 0.211 N/mm for dry samples, and 0.117 to 0.150 N/mm for sealed samples. The noted fracture energy values suggest that the ultimate crack opening displacement could be significantly larger than 25.4 microns. Therefore, using 25.4 microns as a design limit would retain sufficient residual strength to sustain further monotonic or cyclic loading on the cement material.

It is important to point out that the post-cracking design concept acknowledges that the limited cement cracking displacement is acceptable, providing the design forces are displacement-controlled and bounded. Since the well thermal strains and formation movements are controlled and bound by the magnitude of the well temperature and production conditions, it is suitable to use of post-cracking design concept for thermal well cements.

4. CEMENT CONSTITUTIVE MODELS

Use of the post-cracking design concept requires an advanced FEA model which is capable of capturing the three-dimensional stress/strain conditions, initial elastic response described by Young's modulus and Poisson's ratio, thermal expansion of the material, non-linear stress-strain relationships under compressive loading, cracking and crack propagation under a tensile stress condition and cyclic loading responses.

The fracture mechanics based FEA approaches proposed by Hillerborg et al. (1976) have been implemented in some FEA programs. For example, the commercial FEA program ABAQUS (2013) has implemented the smeared cracking model and damaged plasticity model, based on Hillerborg's theory. As mentioned earlier, Xie et al. (2011) used a smeared cracking model to investigate the impact of heating rate on the cracking potential of the cement sheath during the heating phase for SAGD wells. The smeared cracking model consists of an isotropically-hardened yield surface that is active when the stress is dominantly compressive and an independent "crack detection surface" that determines if a point fails by cracking. It is designed for applications in which the cement or concrete is subjected to essentially monotonic straining at low confining pressures.

Furthering the smeared cracking model, a damaged plasticity model is recommended in order to better capture the thermal-mechanical behavior of cement in thermal wells, especially under cyclic thermal-mechanical loading (Xie 2014a). The damaged plasticity model uses concepts of isotropic damage in the elastic behavior in combination with isotropic tensile and compressive plasticity to represent the inelastic behavior of cement. This plasticity-based damaged model assumes that the main two failure mechanisms are tensile cracking and compressive crushing. It consists of the combination of non-associated multi-hardening plasticity and scalar damage in the elastic behavior to describe the irreversible damage that occurs during the fracturing process. The model is designed for applications in which cement or concrete is subjected to monotonic, cyclic and/or dynamic loading under low confinement. A similar damaged plasticity model for concrete was developed by Xie et al. (1996), with the consideration of high confining stress effects.

As shown in Figure 1a), under uniaxial tension, the stress-strain response follows a linear elastic relationship until the value of the failure stress(σ_{t0}) is reached. The failure stress corresponds to the onset of micro-cracking in the concrete material. Beyond the failure stress, the formation of micro-cracks is represented with a softening stress-strain response. Under uniaxial compression, as shown in Figure 1b), the response is linear until the value of initial yield. In the plastic regime, the response is typically characterized by stress hardening, followed by strain softening (beyond the ultimate stress (σ_{c0})).This representation, although somewhat simplified, captures the main features of the response of cement.

When the cement material is unloaded from any point on the strain softening branch of the stress-strain curves, the unloading response is weakened, represented by the degradation of the elastic modulus. Two damage variables (d_t and d_c) are used to describe the degradation of the elastic modulus in tension and compression. These two damage variables are assumed to be functions of the plastic strains' temperature and field variables. For the cyclic loading analysis, the stiffness recovery effect associated with stress reversal (i.e. crack closing) is considered by introducing stiffness recovery factors.

The same concepts for the damage variables and stiffness recovery factors are used for the multi-axial mechanics modeling.

5. ANALYSIS EXAMPLE

An illustrative scenario for a SAGD well was analyzed using the damaged plasticity model for a cement sheath. The case was analyzed to study the impact of steam heating rate on cement cracking and the impact of cooling phase on potential de-bonding.

5.1 Structural and Material Models

Figure 4 shows the FEA model, using axisymmetric solid elements. The model included intermediate and surface casing strings, cement sheaths and surrounding formations.

To accurately capture the temperature distribution field around the well, the model used a mesh density of one element per meter along the axial direction. In the radial direction, ten elements were used for each of the casing and cement layers and more than 30 elements of increasing radial thickness for the formations.

The example considers a well with an overburden thickness of 360 m and caprock thickness of 10 m. The overburden is assumed to have properties that change linearly with depth from surface to the top of the caprock with the elastic modulus of 100 MPa to 1.35 GPa, thermal expansion coefficient of 2.0×10^{-6}/°C to 1.6×10^{-6}/°C, initial temperature of 4°C to 9°C and thermal conductivity of 2.0 W/m·K to 1.7 W/m·K.

The caprock has an elastic modulus of 1.19 GPa, thermal expansion coefficient of 5.0×10-6/°C, initial temperature of 10°C and thermal conductivity of 1.7 W/m·K.

The injection well is completed with a surface casing of 406.4 mm (16 in), 96.7 kg/m (65 lb/ft) H40 casing material landed at 150 m MD in a 508.0 mm (20 in) hole; an intermediate casing of 298.5 mm (11.75 in), 69.9 kg/m (47.0 lb/ft) L80 casing material landed at 750 m MD in a 374.5 mm (14.75 in) hole and a horizontal liner of 219.1 mm (8.625 in), 47.6 kg/m (32 lb/ft) 820 m in length with the liner hanger at 740 m MD in a 269.9 mm (10.625 in) hole. The steel materials are assumed to have an elastic modulus of 200 GPa, thermal expansion coefficient of 12×10^{-6}/°C and thermal conductivity of 45 W/m·K.

The surface and intermediate cement sheaths are modeled using the damaged plasticity model. The cement is assumed to have the elastic modulus of 8.5 GPa, compressive strength of 48 MPa, tensile strength of 4.8 MPa, thermal expansion coefficient of 9.0×10^{-6}/°C and thermal conductivity of 1.0 W/m·K. In defining the damaged plasticity model, the fracture energy is assumed to be 0.15 N/mm. Assuming a linear tensile stiffening curve, the critical crack displacement at zero tensile stress is determined to be 0.0625 mm. The damage variables are assumed to be 0.9 at the critical cracking displacement for tension and at the critical crushing strain for compression. The stiffness recovery ratios are assumed to be 0.2.

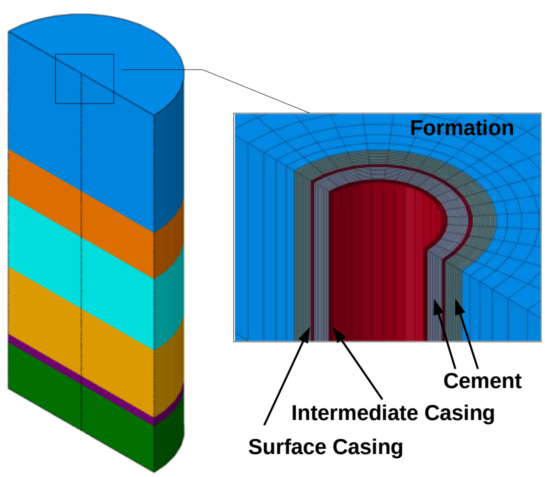

Figure 4 FEA Model showing Various Formation Layers (left) and Wellbore (right).

5.2 Modeling of Thermal Loading in Heating Phase

The analysis focused on the impact of the heating rate during the heating phase. Seven heating rates from 0.15°C/min to 5°C/min were analyzed. The peak steam temperature was assumed to be 220°C and the initial temperature was 5°C. The relationships between the casing ID temperature and time are shown in Figure 5.

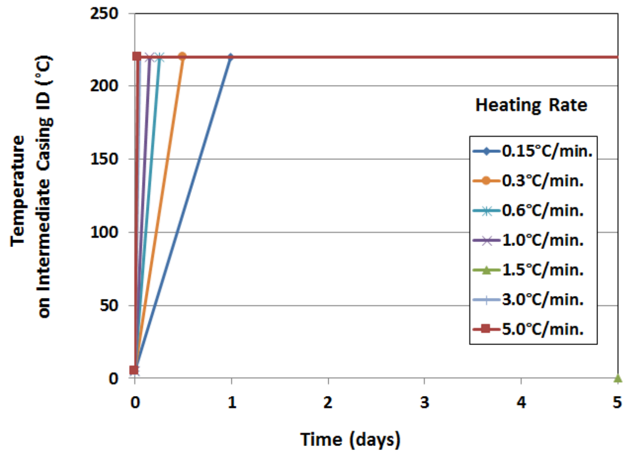

Figure 5 Various Heating Rates Considered in Analysis

The heating phase was analyzed in two steps. First, an equilibrium stress state condition was applied using geostatic analysis to consider the effect of the weight of the overburden and caprock. Secondly, a coupled thermal-displacement analysis was performed to determine, as a function of time, the temperature distributions around the wellbore and the stresses and deformations in the casing strings and cement sheaths that result from material thermal expansion and formation confinement.

Figure 6 presents the contour plots of temperature and tensile damage variable in the casing, cement and formation. This is shown in the caprock interval after 5 hours, 2 days and 1 year of heating for the well subjected to the base case heating rate (0.6°C/min.). The intermediate casing reaches a relatively uniform temperature along the full length of the wellbore; however, a significant temperature gradient from the casing to the outer surface of the cement sheath and out from the wellbore into the formation was found even after one year of heating.

The cement cracking is caused by the various thermal expansion amounts of the casing, cement and formation materials. The immediately-heated intermediate casing would expand to cause high circumferential stress in cement sheath. As shown in Figure 6, the temperature decreases through the cement thickness. As a result, the cement portion adjacent to the casing would expand further and the initial cracking would develop in the cement portion adjacent to the formation.

Figure 7 presents the history of the crack displacement over the caprock interval for the seven heating rates from 0.15°C/min to 5°C/min studied. It shows that cracks develop in the cement in the early stages of heating when the temperature gradient is high. Heating for several days tends to warm up more cement and formation volumes and slows down the further cracking. The magnitude of the cement crack displacement increases with quicker heating rates.

After five days of heating, the crack displacement values are 8.5, 13, 19.5, 25.1, 30.5, 38 and 42.5 microns for the heating rates of 0.15°C/min, 0.3°C/min, 0.6°C/min, 1.0°C/min, 1.5°C/min, 3.0°C/min and 5.0°C/min, respectively. Assuming that a threshold value of crack displacement is set as 25.4 microns, the highest allowable heating rate would be approximately 1.0°C/min.

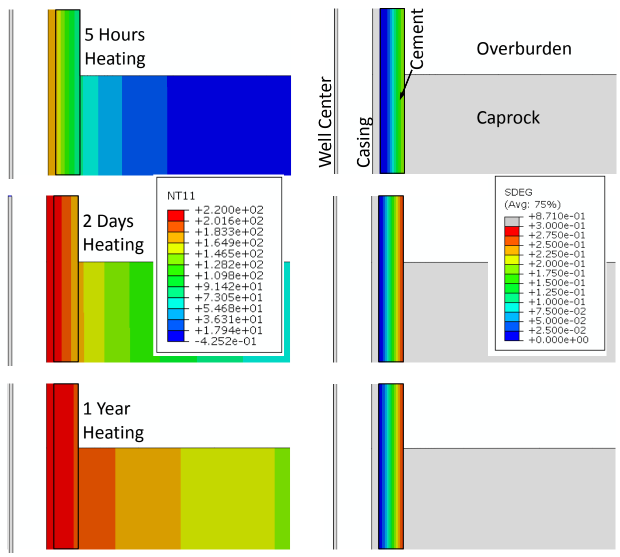

Figure 6 Temperature (°C) Profile (Left) and Tensile Damage Variable (Right) for the Base Case during Heating

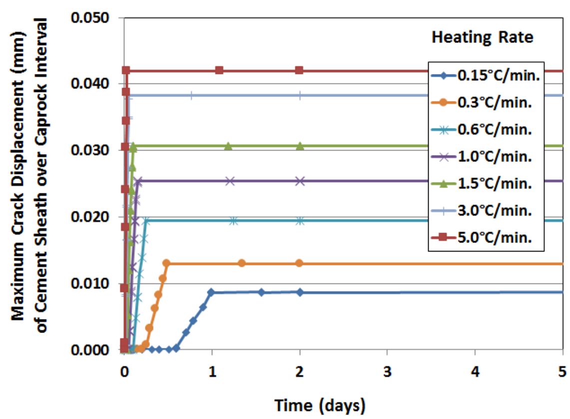

Figure 7 Maximum Cement Crack Displacement

5.3 Modeling of Cooling

For the cooling phase, a steady state analysis was performed to determine the impact of heat dissipation to the surrounding formations on the cement mechanical behavior. Since the steady state analysis was performed, cooling time was not specifically defined. Instead, analysis results are presented in terms of casing ID temperatures. Figure 8 presents the temperature distribution and radial stress in the cement sheath corresponding to the casing ID temperatures (over caprock interval) of 220°C, 109°C and 38°C during the cooling phase. The non-uniform temperature distribution in the casing and cement causes a decrease in the compressive radial stress in the cement sheath next to the casing OD. The radial compressive stresses in the cement next to the casing are 5.35, 3.59 and 2.37 MPa, corresponding to the casing temperatures of 220°C, 109°C and 38°C. If the radial stress in the cement changes from compression to tension, de-bonding between the cement and casing occurs. The results suggest that the cooling phase increases the potential for de-bonding between the casing and cement; however, in this case, the de-bonding does not occur even at 38°C casing ID temperature during cooling.

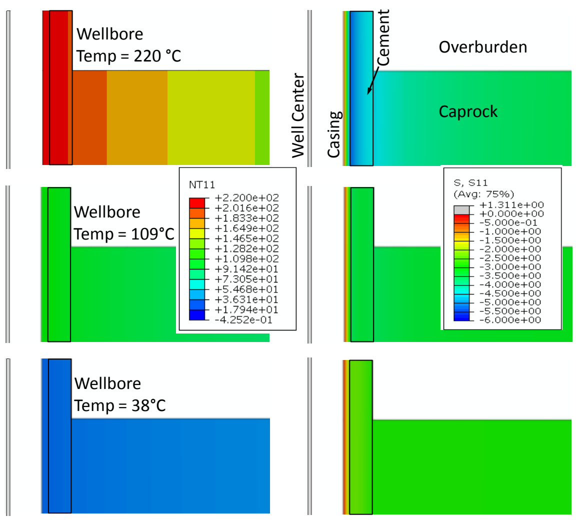

Figure 8 Temperature (°C) Profile (Left) and Radial Stress (MPa, Right) for the Base Case during Cooling

6. CONCLUSIONS

This paper presents a review of cement mechanical properties and proposes a new design basis for thermal well cements: post-cracking design concept. A damaged plasticity model is recommended for analyzing the thermal-mechanical behavior of cement in thermal wells. The proposed analysis and design approach is demonstrated by analyzing an illustrative scenario of a SAGD well.

The following conclusions are made:

- Post-cracking design concept is proposed as a new design basis for cement in thermal wells. The post-cracking design allows for limited cement cracking, providing that the permeability of the cement does not increase beyond acceptable values. A threshold of 25.4 micron is recommended as the crack displacement limit for cement design.
- The damaged plasticity model considers the tri-axial stress effect, strain-hardening due to plasticity, strain-softening due to cracking and cyclic loading. It is a robust numerical tool for analyzing cement behavior in thermal wells.
- An illustrative scenario case was analyzed under the thermal mechanical loading resulting from the heating and cooling operations of a SAGD well. The analysis demonstrated that quicker heating rates tend to increase the potential of cement cracking. For the cooling phase, the potential for de-bonding between the casing and the cement increases as the wellbore temperature decreases with cooling time.

7. NOMENCLATURE

d_t = Degradation of the elastic modulus in tension
d_c = Degradation of the elastic modulus in compression
E_c = Elastic modulus
f_t' = Tensile strength
f_c' = Compressive strength
G_f = Fracture energy
u_{cr} = Crack displacement
ν = Poisson's ratio

8. REFERENCES

1. ABAQUS. (2013). User's Manual. (Version 6.13).
2. Abdoulghafour, H., Luquot, L. and Gouze P. (2013). Characterization of the Mechanisms Controlling the Permeability Changes of Fractured Cements Flowed Through by CO2-Rich Brine. Environment Science & Technology, 47 (18), 10332-10338.
3. Akhavan, A., Shafaatian, S.M.H., Ajabipour, F. (2012), Quantifying the effects of crack width, tortuosity, and roughness on water permeability of cracked mortars, Cement and Concrete Research, 42, 313-320.
4. Alberta Energy Regulator. (1990, July). Directive 009: Casing Cementing Minimum Requirements.
5. Bosma, m., Ravi, K., Van Driel, W. and Schreppers, G.J. (1999, Oct. 3-6). Design approach to Sealant Selection for the Life of the Well. SPE Annual Technical Conference and Exhibition, Houston, TX, USA. SPE 56536.
6. Dean, G. D., Torres, R. S. (2002). Novel Cement System for Improved Zonal Isolation in Steam Injection Wells. SPE/Petroleum Society of CIM/CHOA 78995.

7. Debruijin, G., Garnier, A., Brignoli, R., Bexte, d., and Reinheimer, d. (2009, March 17-19). Flexible Cement Improves Wellbore Integrity in SAGD Wells. SPE/IADC Drilling Conference and Exhibition, Amsterdam, The Netherlands, SPE/IADC 119960.
8. Hillerborg, A., Modeer, M. and Peterson, P-E. (1976). Analysis of Crack Formation and Crack Growth in Concrete by Means of Fracture Mechanics and Finite Elements. Cement and Concrete Research, Vol. 6, 773-781.
9. Macharia, m. m., Sato, R., Shigematsu, A. and Onishi, H. (2011, Aug. 14-16). Study of Fracture Energy Properties of Portland Blast Furnace Cement Type-B Concrete with Partial Replacement of Aggregate Porous Ceramic Course Aggregate. 36th Conference on Our World in Concrete & Structures, Singapore.
10. MacGregor, J. G. (1992). Reinforced Concrete – Mechanics & Design. (2nd ed.). Prentice Hall.
11. Padevet, P. and Zobal, O. (2011, Sept. 20-22). Fracture Energy of Cement Paste with Addition of the Fly Ash. Modeling of Mechanical and Mechatronic Systems, 4th International Conference, Herlany, Slovak Republic.
12. Ravi, K., Hunter, B. and Kulakofsky, d. (2008, March 10-12). Job Design and Cement System to Contain Steam and Improve Heavy Oil Recovery. World Heavy Oil Congress 2008, Edmonton, AB, Canada. WHOC 2008-381.
13. Stiles, D. (2006, Feb. 21-23). Effects of Long-Term Exposure to Ultrahigh Temperature on the Mechanical Parameters of Cement. Miami, Florida. IADC/SPE 98896.
14. Thiercelin, M.J., Darguad, B., Baret, J.F. and Rodriguez, W.J. (1997, Oct. 5-8). Cement Design Based on Cement Mechanical Response. SPE Annual Technical Conference and Exhibition, San Antonio, TX, USA. SPE 38598.
15. Walsh, S. d. C, Du Frane, W. L., Mason, H. E. and Carroll, S. A. (2013). Permeability of Wellbore-Cement Fractures Following Degradation by Carbonated Brine. Rock Mech Rock Eng 46, 455-464.
16. Wang, K., Jansen, D.C., Shah, S.P. (1997), Permeability study of cracked concrete, Cement and Concrete Research, 27, 381-393.
17. Xie, J., Elwi, A.E. and MacGregor, J.G. (1995). The Mechanical Properties of Three High Strength Concretes Containing Silica Fume. ACI Material Journal, Vol. 92, No. 2, March-April, 135-145.
18. Xie, J. Elwi, A.E. and MacGregor, J.G. (1996). Numerical Investigation of Eccentrically Loaded High-Strength Concrete Tied Columns. ACI Structural Journal, July-August, 449
19. Xie, J. and Zahacy, T. (2011). Understanding Cement Mechanical Behavior in SAGD Wells. World Heavy Oil Congress, Edmonton, Alberta. WHOC11-557.
20. Xie, J., (2014a), Analytical Modeling of Cement Mechanical Behavior in Thermal Wells. World Heavy Oil Congress, New Orleans, USA. March 5-7. WHOC14-104.
21. Xie, J. (2014b), Post-Cracking Design for Thermal Well Cements. SPE Thermal Well Design and Integrity Workshop. Banff, Alberta, Canada. November 18-20.
22. Xie, J. (2015), Reliability-Based Design and Assessment (RBDA) with Post-Cracking Design Basis for Thermal Well Cements. World Heavy Oil Congress, Edmonton, Canada. March 24-26. WHOC15-108.

9. ACKNOWLEDGMENTS

The funding for preparing this paper was provided by C-FER Technologies. The author would like to acknowledge Dr. Feng Rong, Research Engineer at C-FER Technologies for assistance in the numerical modeling.